Published in: Mater. Sci. Eng. A, 491, 2008, 279-289

Thermal activation of fatigue crack growth: analysing the mechanisms of fatigue crack propagation in superalloys

M.J. Starink* and P.A.S. Reed

Materials Research Group, School of Engineering Sciences, University of Southampton, Southampton SO17 1BJ, UK

ABSTRACT

A method for deriving apparent activation energies, E_{app}, for fatigue crack growth (FCG) is presented. It is shown how these E_{app} values can be used to analyse the main underlying mechanism causing the progression of the crack. The E_{app} values for fatigue crack growth in air and vacuum, and with and without a dwell are obtained for a range of Ni based superalloys for turbine disc applications. The apparent activation energies range from about zero to about 300kJ/mol. The analysis allows identification of alloys that are prone to FCG through diffusion controlled mechanisms, notably grain boundary oxidation or grain boundary creep, as well as alloys that are nearly immune to FCG by grain boundary oxidation or creep.

1. INTRODUCTION

In many engineering applications where conditions involve high temperatures and cyclic stresses, creep-fatigue and/or oxidation-fatigue can be the main cause of failure. Optimising materials in terms of such time-dependent fatigue resistance is complex, not least because the unambiguous determination of which processes are in operation is challenging. A wide range of operating conditions (temperature, environment, loading cycle shape, strain rate, dwell time) need to be assessed in terms of both the effect on crack propagation rates (either in terms of da/dN or da/dt) and also which crack driving force is in operation and best describes that crack propagation (e.g. stress intensity factor, ΔK, the J-integral, ΔJ, the C-integral, C^*, [1] etc). Once the crack growth rate behaviour is characterised adequately, then further materials optimisation requires the mechanisms of failure in operation to be determined. Usually this is attempted by a combination of post-failure fractographic analyses and crack propagation comparisons, where key parameters have been varied explicitly. Since failure is multi-mechanistic, to clearly define the dominant or rate-determining process can be complex and open to many alternative interpretations. Not least because the testing requirements themselves are challenging with many possible parameters that need to be considered. In-situ observation techniques (e.g. characterisation of cracks during crack growth using X-ray tomography [2,3]) may offer new insights, but the challenges of experimental set-up,

resolution issues, etc, mean that the most complex (and usually service relevant) conditions are unlikely to be assessable by such methods. It is clear then that the ambiguities inherent in such a complex problem mean that better data analysis approaches are needed to compare across alloy systems and testing conditions to allow us to pick out the key microstructural features that will lead to optimised behaviour.

Thus it will be of great benefit to explore a complementary technique that aids interpretation of these complex fatigue crack growth (FCG) experiments, and that can be used to critically assess the interpretations and suggestions derived from existing techniques. The present paper provides a methodology for derivation and application of an analysis method of the thermal activation energy for fatigue that is significantly expanded vis-à-vis some limited early work in the field [4,5,6]. The technique requires FCG data from at least two temperatures (in the regime of interest) obtained under otherwise identical testing conditions. These data are used to calculate an (apparent) activation energy, E_{app}, for FCG and these are then compared both between alloys and testing conditions and compared with known activation energies for basic damage processes such as grain boundary creep and oxidation. In the present paper we will limit ourselves largely to presenting and illustrating this new method; and apply it to Ni based superalloys.

The generic method will be illustrated through application to alloys for gas turbine disc applications. Gas turbine discs experience differing service conditions across the component ranging from temperatures of around 300°C and relatively high stresses at the bore to higher temperatures of around 650°C and somewhat lower stresses at the rim. Stress concentration features such as fir tree root fixings at the rim increase the need for excellent high temperature damage tolerance in view of the cyclic loading experienced by these components [7]. Most turbine discs are now manufactured from Ni based superalloys due to their good resistance against combinations of fatigue, creep, oxidation and corrosion damage. The overall performance of aero- and utility gas turbines is determined by the maximum operating temperatures possible for these Ni based superalloy components and fatigue crack propagation (FCP) is in many cases considered the main limiting property.

At higher temperatures, above 500°C, FCP in Ni based superalloys is temperature and time dependent. The mechanisms responsible for this temperature and time dependency have been discussed in a range of works (see e.g. [8,9,10,11,12,13,14,15,16,17,18,19] and references therein). Generally 3 main groups of mechanisms are cited for this temperature dependence: i) environmental effects including dynamic embrittlement involving atomic oxygen [8,9] and/or oxidation of grain boundaries, γ' ($Ni_3(Al,Ti)$) [19] and grain boundary carbides [13,14] (the latter two processes are stress assisted), ii) creep (especially at grain boundaries) and iii) changes in the monotonic mechanical properties of the material, most notably the yield strength. There is no doubt that all of

these mechanisms occur in superalloys, however it is not straightforward to determine which mechanism is dominant in any particular alloy. Understanding which of these mechanisms is dominant is crucial to improving these safety critical components.

2. ANALYSIS METHOD: THE ACTIVATION ENERGY FOR FATIGUE CRACK PROPAGATION.

There are several ways to derive the same basic recipe for obtaining an apparent activation energy from FCP data. We will present a detailed derivation, which is in part inspired by activation energy analysis methods used for solid state reactions (see e.g. [20,21,22,23]). We consider that the progress of many processes is dominated by a thermally activated reaction such that the rate is proportional to an Arrhenius term:

$$\frac{d\alpha}{dt} \propto k\, f(\alpha) \exp\frac{-Q}{R_g T} \tag{1}$$

Where dα/dt is the rate of transformation, T is the temperature, Q is the activation energy, and R_g is the gas constant (8.31 J/mol.K), f is a function depending only on the extent of the reaction completed, k is a term that contains all terms that do not depend on T, t and α. The process involved can be thermally activated dislocation motion (including creep), solid state reactions, gas-solid reaction (including oxidation), diffusion, and a range of less relevant processes. In applying this notion to FCP we can thus state that for the evolution of the crack length, a, the rate equation is:

$$\frac{da}{dt} \propto k_{FCG} f(a) \exp\frac{-Q}{R_g T} \tag{2}$$

where k_{FCG} is a term that contains all non temperature dependent terms, except for the length of the crack, for FCP this would include terms related to the loading cycle (e.g. range of crack tip stresses (e.g. ΔK), stress ratio R), the microstructure, monotonic mechanical and deformation properties, etc. The general way in which the product $k_{\mathrm{FCG}}\, f(a)$ is kept constant is by defining a crack driving force such as ΔK, ΔJ ,or C^* appropriate for the material's loading condition [1]. Thus, if the product $k_{\mathrm{FCG}}\, f(a)$ is kept constant, we can obtain the (apparent) activation energy, E_{app}, from two FCG tests at two temperatures, T_2 and T_1, using:

$$E_{app} = \frac{-R_g}{T_2^{-1} - T_1^{-1}} \ln\left(\frac{da}{dt}(T_2) \Big/ \frac{da}{dt}(T_1) \right) \tag{3}$$

In this approach the loading cycles at the two temperatures are identical, and hence da/dt is proportional to da/dN. We may thus write:

$$E_{app} = \frac{-R_g}{T_2^{-1} - T_1^{-1}} \ln\left(\frac{da}{dN}(T_2) \Big/ \frac{da}{dN}(T_1) \right) \quad (4)$$

This formulation can be applied directly to a range of data sets. For instance, if ΔK is a good description for the crack driving force, da/dN vs. ΔK curves obtained at two temperatures (such as the ones plotted in Fig. 1 can be used.

To further elucidate the physical meaning of the activation energy we may formulate this in an alternative way. Whilst holding all other test conditions constant, determine the times, t_2, and t_1, needed for the crack to grow a fixed length at two temperatures T_2 and T_1. Then the activation energy is given by:

$$E_{app} = \frac{R_g}{T_2^{-1} - T_1^{-1}} \ln\left(t_2 / t_1\right) \quad (5)$$

This formulation is reminiscent of the concept of 'equivalent state' [21,22] achieved in a process, i.e. we define an equivalent state to be reached during the process (here a length of fatigue crack propagation, or new interface to air produced by FCP) and measure the times needed at two temperatures whilst holding all other experimental conditions constant.

This approach is consistent with the case of creep being a dominant process, as in that case we could anticipate that:

$$\frac{d\varepsilon}{dt} = A\left(K_{\max}\right)^n \exp\frac{-Q}{R_g T} \quad (6)$$

where ε is a creep deformation responsible for failure, n is the stress exponent characteristic for the creep mechanism concerned (see e.g. [24]).

Whilst the derivation of this method follows the concept of activation energy analysis for thermally activated reactions [20,21,22], it is important to note that application to FCG will lead to a set of issues that unknown or very rare in thermally activated reactions. Firstly, FCG may show little or no temperature dependency over a large range of temperatures. For instance, most FCC superalloys will not suffer from oxidation or creep, or undergo a substantial change in monotonic mechanical properties, over temperature ranges from about -100 to 400°C, whilst at elevated temperatures, typically in the range of about 600 to 800°C FCG rates in air will drastically increase with increasing temperature, due to thermally activated processes. (We may term fatigue that is not directly related to a thermally activated process 'mechanical fatigue'.) So the apparent activation energy will be zero at low temperatures, and change to a substantial value (below we will show that this can be 100-350kJ/mol) that is determined by the underlying dominant thermally activated

processes. There are at least four distinct thermally activated processes involved in FCG: i) localised oxidation at and ahead of the crack tip, ii) dynamic embrittlement [8], iii) creep, which may be localised at ligaments or at grain boundaries and iv) thermally activated modes of dislocation movement, which may influence, amongst others, the temperature dependence of the monotonic mechanical properties. The relative importance of these processes can change with temperature and crack tip stress cycle, and thus apparent activation energies will change depending on these parameters, especially in conditions that are important in high temperature applications, i.e. when the FCG resistance starts to deteriorate due to environmental and stress conditions. Activation energies for FCG will thus generally be dependent on temperature. This is different from some other thermally activated reactions, where the activation energy generally undergoes little change with temperature [25].

The above is formulated on the basis of two test temperatures, T_1 and T_2, providing one apparent activation energy. With activation energies likely to change with temperature, we would ideally wish to obtain data on FCG rates at a large range of temperatures. However it is relevant to consider experimental limitations, and consider i) how many different tests at different temperatures are needed to provide a meaningful analysis and ii) at which temperature intervals these tests would need to be conducted. As to the latter point, we need to consider that FCG propagation data tends to have a substantial scatter. In practice this means that $\left| T_2 - T_1 \right|$ needs to be sufficiently large. From comparison of duplicate tests for a range of superalloys we estimate that in order to achieve an accuracy of about 50kJ/mol, $\left| T_2 - T_1 \right|$ needs to typically be at least about 50K. As temperature ranges of interest in typical applications are often smaller than 100K, there is thus a balance that needs to be negotiated: small temperature intervals allowing 3 or more tests over a range of about 100K will provide more activation energies, but at a lower accuracy (possibly enticing erroneous conclusions on temperature dependence of apparent activation energy); whilst using only 2 points will provide a greater accuracy, but not allow any analysis of temperature dependence of activation energy. There are also implications in terms of time and costs in expanding the number of temperatures; and if time and funds allow more expansive test matrices it is often more fruitful to vary loading cycles or environment. This combination of experimental scatter, external limitations (cost, time) and competing testing options (loading cycles, environment) means that in practice there is a combination of strong drivers which limit the number of temperatures considered. The experiments reported and analysed in this work were conducted over the past 3 decades, and were not designed for systematic analysis of activation energies. On very rare occasions tests at 3 or more temperatures are reported, but the majority of the data considered contains only two test temperatures.

Fig. 1. FCG rates, d*a*/d*N*, as a function of Δ*K* for U720Li-LG at two temperatures, for 1-1-1-1 and 1-20-1-1 cycles, in air and in vacuum.

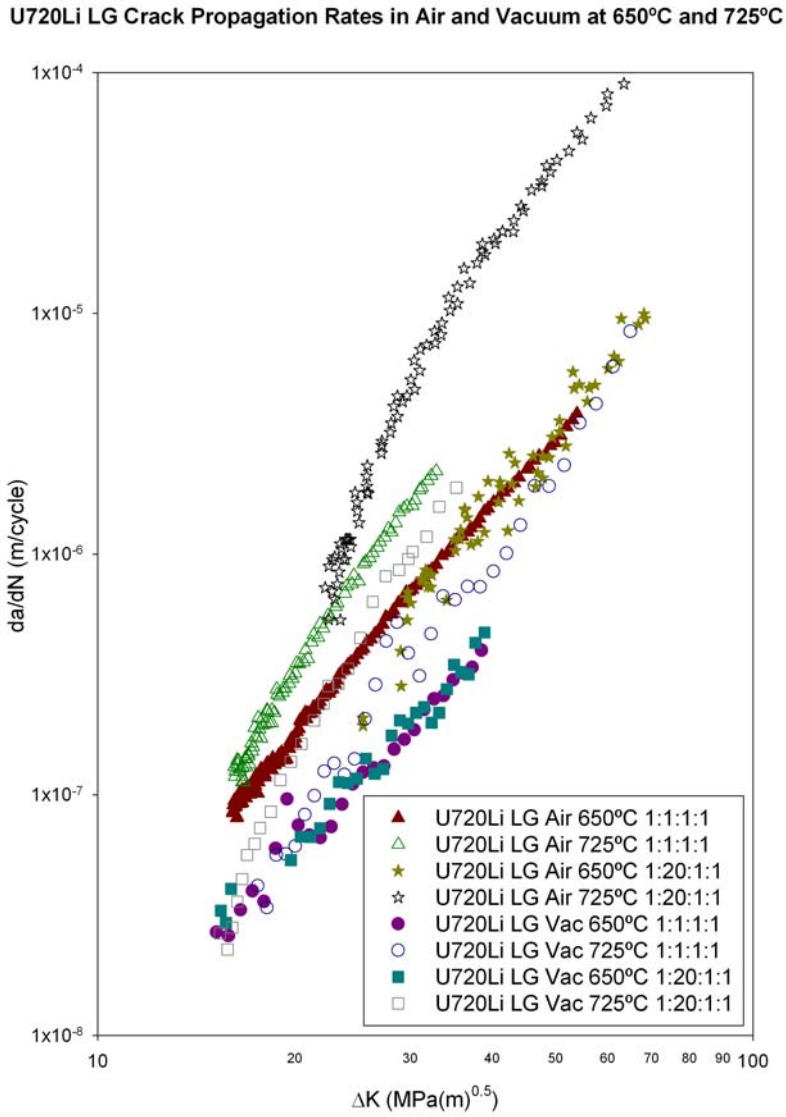

3. MATERIALS, EXPERIMENTAL PROCEDURES, DATA

To investigate the model, FCG data on N18 [26,27], RR1000 [28], Udimet 720 low interstitial (U720Li) [16,17] and U720Li Large Grain (U720Li-LG) variant [27], Waspaloy [29], CH99 [30], Rene95 and Haynes230 [18] are analysed. U720Li is a variant of the U720 alloy designed to minimise the formation of topologically closed packed phases which are detrimental to the properties, and U720Li-LG is an experimental (large grain size) variant produced by solution heat treating U720Li at a somewhat higher temperature. N18 is a powder metallurgy (PM) turbine disc material, developed for the SNECMA M88 engine used in the RAPHALE fighter aircraft, however

it differs significantly from other new generation PM turbine disc alloys in both composition and heat treatment [26,27]. The compositions of the alloys are presented in Table 1 and the heat treatments applied are presented in Table 2. The RR1000 alloy studied is an early generation version of this alloy.

The tests and a detailed description of experimental conditions for testing of N18, RR1000, U720Li and U720Li LG were reported before [16,26,27,31], but we will here summarise the experimental conditions. N18 fatigue testing was carried out using a servo-hydraulic Instron 8501 fitted with a high temperature vacuum chamber. Testing was carried out in three point bend conditions on single edge notched bend specimens (SENB). Fatigue testing of RR1000, U720Li and U720Li LG was carried out using compact test specimens in air and under SENB three point bend conditions in vacuum. For all materials, temperature was monitored and controlled at 650ºC or 725ºC to ± 2ºC, vacuum levels were kept to 1 x 10^{-5} torr. After precracking, cracks were propagated using an initial ΔK of 15 MPa√m using 1-1-1-1 and 1-20-1-1 trapezoidal waveform (0.25Hz), R=0.1, and were allowed to propagate to failure under constant load (increasing ΔK conditions). Crack length was monitored using the direct current (DC) electrical potential (p.d.) difference method and corrected post-test using a linear correction factor obtained from optical measurements of initial and final crack length measurement.

Testing procedures and data for Rene 95 and a CH99 alloy (Ni-11Cr-18Co-2.5Mo-5.5W-3.8Al-3.8Ti-3Ta) were reported by Chang [30]. The CH99 was forged at two different temperatures (1125 and 1175°C) and two different cooling rates (40 and 75°C/min) were applied after the supersolvus anneal at 1200°C. Fatigue tests were conducted on test samples at 650°C and at 760°C. Cyclic stress was applied using a sinusoidal waveform with a three second cycle which was interrupted by a 90 second hold at the maximum stress, with R=0.05.

Table 1 Composition of alloys (in wt %) referred to in this paper. Balance is formed by Ni.

Alloy	Co	Cr	Mo	Al	Ti	Hf	C	B	W	Fe	Zr	Nb	Ta
N18	15.4	11.1	6.44	4.28	4.28	0.50	0.022	0.008	---	---	0.019		---
RR1000	14.0-19.0	14.35-15.15	4.25-5.25	2.85-3.15	3.45-4.15	0.5-1.0	0.012-0.033	0.01-0.025	---	0.0-1.0	0.05-0.07		1.35-2.15
U720Li&LG	14.6	15.9	2.98	2.44	5.18	---	0.023	0.016	1.35	0.08	0.042		---
Rene95	8.0	13.0	3.5	3.5	2.5	---	0.06	0.01	3.5	---	0.05	3.5	---
CH99	17-19	10-12	1.5-3.5	3.25-4.25	3.25-4.25	---	<0.1	0.005-0.03	4.5-6.5	---	0.02-0.08	---	2.5-3.5
Waspaloy	13.5	19.6	4.3	1.37	2.95	---	0.019	0.0063	---	---	0.06		---
Haynes230	5	22	2					0.01	14	3			
DS GTD111	9.0-10.0	13.7-14.3	1.4-1.7	2.8-3.2	4.7-5.1	---	0.08-0.12	0.005-0.020	3.5-4.1	<0.3	0.005-0.040		2.5-3.1
In718*	0.4	18	3	0.5	1.0		0.03	0.003		19		5	

* typical composition

Table 2 Heat treatments applied to the N18, RR1000, U720Li and CH99 alloys. (* all ageing heat treatments were followed by an air cool)

Alloy	Solution heat treatment		Ageing heat treatments*	
N18	4h 1165°C	air cool	24h 700°C	4h 800°C
RR1000	4h 1120°C	fan air cool	24h 650°C	16h 760°C
U720Li	4h 1105°C	oil quench	24h 650°C	16h 760°C
U720Li LG	4h 1135°C	air cool	24h 650°C	16h 760°C
CH99 optim*	1200°C	10C/min	16h 760°C	

* an optimised heat treatment according to [30]

Testing procedures and data for Waspaloy were reported by Liu et al [29]. In the present work, tests at temperatures 705 and 760 °C with loading cycles consisting of a trapezoid wave with 3s+100s loading at maximum stress are analysed. Testing procedures and data for Haynes230 were reported by Lu et al [18]. In the present work, tests at temperatures 649, 814 and 917°C with loading cycles consisting of triangular waveform with a frequency of 0.333 Hz and R ratio of 0.05 are analysed. Data on FCG in IN718 was obtained from Refs. [32,33].

4. RESULTS

Extensive microstructural data is available for all alloys considered here ([16,17,18,19,26,27,29,30,31,32,33,34] and references therein) and for most alloys fractography data has been published. FCG fractography analysis for N18, RR1000, Udimet 720 low interstitial (U720Li) and U720Li Large Grain (U720Li LG) variant [16,17,26,27] has been interpreted as showing that intergranular failure was promoted in: (1) air *cf.* vacuum, then considering both environments (but to a lesser degree in vacuum): (2) at longer dwells (3) higher temperatures and (4) higher ΔK-levels. In terms of material comparisons, intergranular failure levels varied with grain size, but also with alloy composition and there was a general qualitative correlation between a greater degree of intergranularity observed in the fatigue fracture surfaces and the highest crack growth rates. In this work we will concentrate on the analysis of the activation energies, leaving comparisons with microstructural data and fractography for further work.

In this work we will assume that the crack tip driving force can (at least in good approximation) be described by ΔK, and apply Eq. 2 to FCG data for N18, RR1000, U720Li and U720Li LG for T_2=725ºC and T_1=650ºC for ΔK values of 20, 30, 40 and 50 MPa√m (for the latter 3 alloys data for both air and vacuum experiments is available). The same approach has been applied to IN718, CH99, Waspaloy and Haynes230 tested under various conditions for ΔK values between 20 and 50 MPa√m. The obtained activation energy values are plotted in Fig. 2. As expected (see next section), the activation energies cover a wide range: values from -50 to about 350kJ/mol are measured.

Fig. 2. Apparent activation energies for FCG in air and vacuum of a range of Ni based superalloys. For details on experimental conditions see Section 3. (vac stands for vacuum, (Sad) refers to [33], [Val] refers to [32]).

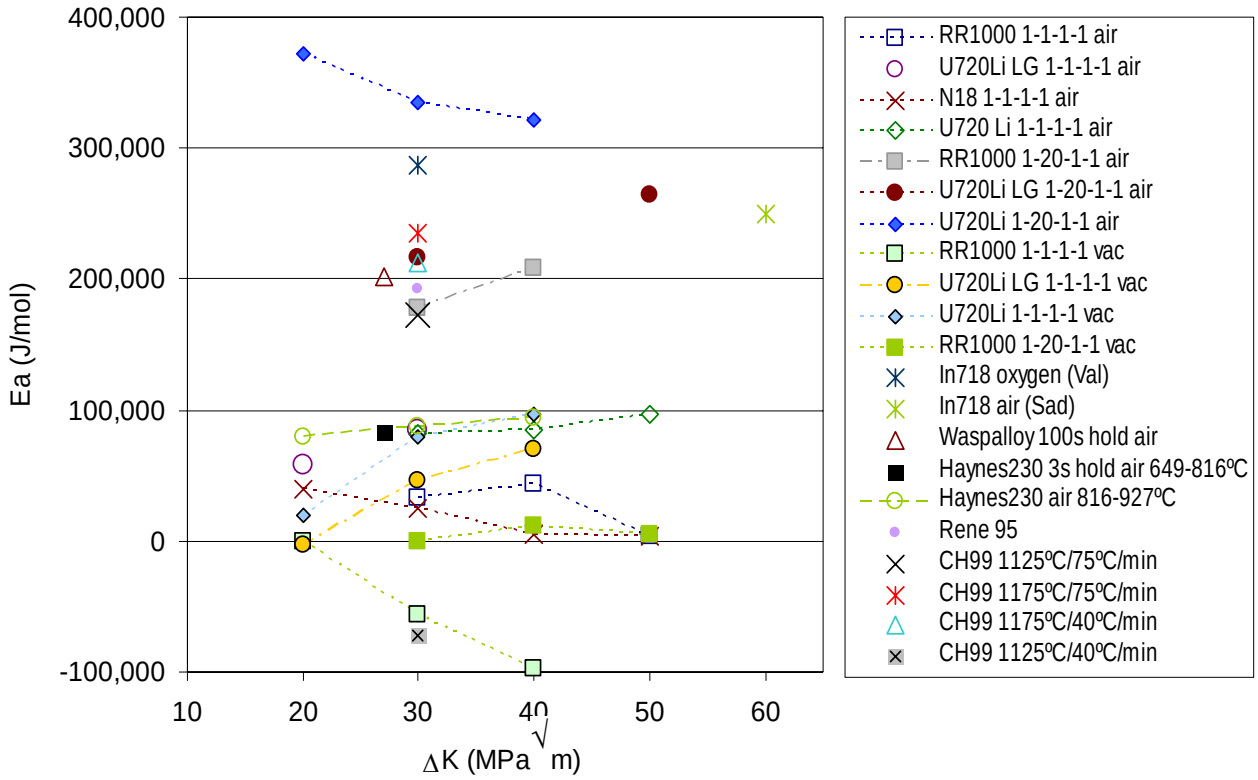

Fig. 3. Radar plot of apparent activation energies for FCG for 3 materials tested in air or vacuum and under 1-1-1-1 or 1-20-1-1 loading at ΔK= 30MPa√m.

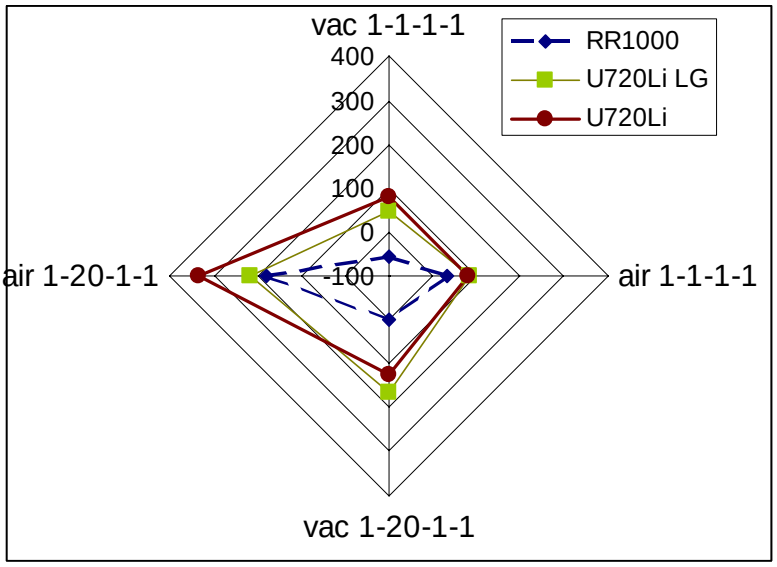

(Negative activation energy means that the FCG rate decreases with increasing temperature; the causes for this are further discussed in Section 6.) For most alloys, the apparent activation energies for air tests increase drastically if a dwell at high stress is introduced and decrease if the test is conducted in vacuum. As activation energies may depend on a range of parameters (ΔK, cycle, R, dwell, test atmosphere, T) many different ways of plotting the data are possible. We here propose a radar plot elucidating the effect of air/vacuum and dwell on the apparent activation energies. Such a plot is provided for 3 alloys in Fig. 3 which pulls out the relative contributions of the different loading and environment conditions across the test matrix very clearly.

5. ACTIVATION ENERGIES OF FUNDAMENTAL DAMAGE PROCESSES IN HIGH TEMPERATURE FATIGUE

To further the analysis of the activation energies obtained, they need to be compared with typical energies for basic processes in superalloys. In this section we will consider the activation energies of the individual processes.

Mass transport by diffusion

For bulk diffusion of metallic alloying elements in Ni, the activation energies are typically between 210 and 300 kJ/mol [34,35,36], Ni self diffusion has an activation energy of about 285 kJ/mol [35,37], whilst the activation energy for C diffusion in Ni is about 140 kJ/mol.

Creep

Experimental analysis of creep data on superalloys indicates activation energies for creep of smooth samples are typically between 280 to 320 k J/mol [38,39,40]. However, for FCP tests where creep is a significant component (i.e. creep-fatigue failure) it is more relevant to consider creep at grain boundaries. Grain boundary sliding can be represented by atomistic models for superplastic flow where sliding along the grain boundaries may be controlled by diffusion flow accommodation within the grain interiors, as in Ashby and Verrall's model [41], or by dislocation climb within the boundary planes, as in Gittus' model [42]. In the first case the temperature dependency will be caused by diffusion within grains and in the latter case by grain boundary diffusion. A model for high temperature deformation of a P/M Rene 95 alloy puts the activation energy for diffusion within grains at 318 kJ/mol and the activation energy for grain boundary diffusion at 159 kJ/mol [43]. Comparisons of flow stress data at 1050°C for P/M 713 LC and P/M Rene 95 with multimechanistic models indicates that at about 1050°C the best predictions are obtained through inclusion of Gittus' model of dislocation climb within the boundary planes, rather than Ashby and Verrall's model of diffusion flow accommodation within the grain interiors [43]. This work [43] indicates that at higher temperature of 1100°C the diffusion flow accommodation within the grain interiors becomes important. In the FCG studies considered in the present paper the temperature is

well below 1000°C and hence for any creep, dislocation climb within the boundary planes should be the dominant mechanism. This assessment is consistent with work by Wu et al. [44], who showed that for a fine grained U738 Ni based superalloy tested at very low strain rates at temperatures between 750 and 950°C, the activation energy for plastic deformation, which should be dominated by grain boundary creep, equals 143kJ/mol. We can thus conclude that the activation energy for creep-dominated FCG should be about 150 kJ/mol.

Creep deformation can be dependent on stress levels. Dislocations interact and mutually impede each others movement, but under an applied stress dislocations can be made to cut through each other generating jogs. In the case of screw dislocations, which are generally considered to be the predominant source for plastic deformation during fatigue, these jogs will restrain further motion and vacancies are needed for continued dislocation motion [6,45]. The energy of formation of a jog, Q_{jog}, is given by [45]:

$$Q_{jog} = \alpha\mu b^3 - \sigma l b^2 \qquad (7)$$

where μ is the shear modulus of the material, l is the length of the dislocation, b is the length of the Burger's vector and α is a constant which has been considered to be about 1. In Ni based superalloys, μ is about 100GPa, b is 0.25 nm, providing a value for Q_{jog} in the limit for low stresses of about 300 kJ/mole, which, as anticipated, is broadly in line with the activation energy for creep of smooth specimens.

Dynamic embrittlement and oxidation

FCG of Ni based superalloys in air has been associated with both dynamic embrittlement involving atomic oxygen being driven into the core of a sharp crack [8,9], and oxidation of particular phases in the alloy [14,46]. In Nb containing superalloys, the oxidation of NbC particles near grain boundaries has been cited as the cause for environmental sensitivity of FCG [19]. As other TiC and HfC carbides can also oxidise readily [47,48,49], the mechanism related to oxidation of carbides of various kinds can potentially cause environmental sensitivity of FCG in most superalloys.

Extensive experiments on pure Ni show that the activation energy for formation of a 1 μm thin layer of NiO in the temperature range 600-800 ºC is about 130 kJ/mol [50], and for thicker layers (10 - 30 μm) formed in the temperature range 900-1200ºC the apparent activation energy increases to about 200 kJ/mol. In a study on a Nb containing Inconel superalloy, the activation energy for oxidation of Ni-based superalloys at high temperatures has been reported to be as high as 255 kJ/mol [14]. However, studies on oxidation of directionally solidified GTD-111 and Rene 80 (both are high Cr (>13wt%), and Nb free) the activation energy for oxide formation has been reported to be as low as 78 kJ/mol and 40 kJ/mol, respectively [51,52]. Clearly the activation energy for oxidation depends on temperature and alloy composition. It appears that alloys with a substantial

Nb content have an activation energy for oxidation of about 250 kJ/mol. Elimination of Nb and a high Cr content seems to reduce the activation energy substantially.

Temperature dependence of monotonic mechanical properties

If neither oxidation nor creep are significant mechanisms for FCP, and no other process with an exponential temperature dependency is the main rate determining factor, activation energies would be expected to be very low, as the influence of changing monotonic mechanical properties will be limited. We can show this by considering that the main driver for crack propagation, the change in crack tip opening displacement [53], depends on the Young's modulus, E, and the yield strength according to:

$$\Delta\delta = 0.5\frac{\Delta K^2}{2E\sigma_y} \tag{8}$$

Combining that with the Paris law [1] provides:

$$\frac{da}{dn} = C_1\left[\Delta\delta^{0.5}\right]^m = C_2\frac{\Delta K^m}{\left(E\sigma_y\right)^{m/2}} \tag{9}$$

where m is the Paris law exponent. We thus find:

$$E_{app} = -R_g\frac{d\ln\left(\frac{da}{dn}\right)}{d(1/T)} = R_g\frac{d\left(\frac{m}{2}\ln\left(E\sigma_y\right)\right)}{d(1/T)} = -\frac{mR_gT^2}{2}\frac{d\left(\ln\left(E\sigma_y\right)\right)}{d(T)} = -\frac{mR_gT^2}{2}\frac{\frac{\Delta\left(E\sigma_y\right)}{E\sigma_y}}{\Delta T} \tag{10}$$

With experimental data on properties or predictions of yield strength at temperature using commercially available software, reasonably accurate predictions of E_{app} due to changes in monotonic mechanical properties are possible. We here provide an estimate for superalloys in the temperature range of interest here. An increase in the temperature from 650ºC to 725ºC may lead to a drop in $\sigma_y E$ by about 20% (which will give an effective increase in CTOD of ~ 20%) and for m between 2 and 6 the apparent activation energy would be between 20 and 60 kJ/mol.

Crack closure

One further thermally activated process influencing FCG rates is crack closure [1,54], most notably oxidation induced crack closure (OICC). OICC can become important if the exposure of surfaces to the environment in the wake of the crack leads to (additional) oxidation that causes a substantial volume expansion. Contacting surfaces at the low stress part of the cycle will then effectively shield the crack tip which will experience an altered loading cycle, including a lower ΔK. In most testing conditions, this reduction in ΔK at the crack tip will not be detected as (an apparent) ΔK will be deduced from measured crack length, load and geometries. Within the concepts outlined in Section

2 this means that it will become impossible to define a constant $k_{FCG} f(a)$, and if apparent activation energy are calculate using apparent ΔK values the OICC will introduce a deviation. As oxidation will be thermally activated OICC will cause a negative contribution to the apparent activation energy for FCG. To fully analyse this effect a range of details, such as rate of oxidation of individual phases, their size and location, and their volume expansion, needs to be known. We will here consider just a few limiting cases and general issues. In the case where oxidation in the wake of the crack in the temperature range is very rapid and is essentially completed within a few load cycles, the effect of OICC should be temperature independent, and hence there is no contribution to the apparent activation energy. The opposite limiting case of very slow oxidation will also cause no contribution to the apparent activation energy. Important contributions to the apparent activation energy will only occur if the rate of expansion due to oxidation is significantly temperature dependent in the wake of the crack where closure can occur. In such a case OICC can be expected to lead to a contribution to the apparent activation energy which is dependent on crack growth rate (and hence dependent on ΔK).

Multiple processes

Generally, the dominant process for FCG will be dependent on temperature, and thus measured apparent activation energies can depend on temperature. To illustrate the issues involved we have sketched several possible situations in Fig. 4. In one scenario (scenario A) FCG is not dependent on a thermally activated process up to about 600ºC, where oxidation with an activation energy of 250kJ/mol becomes dominant. (In Fig. 4, the transition is approximated by linearly adding the crack growth rates of the two processes.) In a second scenario (scenario B), FCG is not thermally activated up to about 600ºC where degradation of mechanical properties with an apparent activation energy of 50kJ/mol becomes dominant. In scenario C, FCG is not thermally activated up to about 600ºC where degradation of mechanical properties with an apparent activation energy of 50kJ/mol becomes dominant and oxidation-fatigue with an activation energy of 250kJ/mol becomes dominant beyond 700ºC. If temperature dependency of FCG is measured, this is usually done at 2 to 3 temperatures separated by about 50 to 100 ºC. Fig. 4b serves to illustrate that if data is obtained around temperatures where mechanisms change, apparent activation energies derived from that data will be intermediate between those of the relevant FCG processes. (It should be noted though that to verify these issues, data on FCG rates at 3 or more temperatures would be needed. Very little such data is available in the open literature.) The FCG data for IN718 at 3 temperatures by Sadananda and Shahinian [33], supports that apparent activation energies increase with increasing temperatures.

Comparing E_{app} for the various processes.

The activation energies for processes contributing to high temperature FCG are summarised in Table 3. In real FCG we can expect that whilst in many cases one process will dominate, in other

instances the process can be multimechanistic, with activation energies being some kind of weighted average of activation energies for the individual processes. One scenario for mutimechanistic behaviour is that cracking in a polycrystalline material can be envisaged as crack advance by intergranular decohesion that is constrained by surrounding ligaments that are either cracking at a slower rate or extending by power-law creep [9]. Another scenario leading to multimechanistic behaviour is that boundaries oriented 45º to the main loading direction are most prone to failure by grain boundary creep (because shear stress along these grain boundaries is highest) and thus boundaries at or close to 45º may be failing due to grain boundary creep, whilst other grain boundaries may be failing due to another process, for instance grain boundary oxidation, or a process that is essentially not thermally activated. In the first case (mixed dynamic embrittlement on grain boundaries – creep of ligaments) activation energies would be around 250kJ/mol as both creep and embrittlement on grain boundaries would have activation energies around that value. In the second case (mixed grain boundary creep-oxidation dominated FCG) activation energies would be between 150 and 250kJ/mol, and in the third case (mixed grain boundary creep-non thermally activated) activation energies would be between 0 and 150kJ/mol. Yet another case, which should be rare, would occur if grain boundary creep and grain boundary oxidation (or dynamic embrittlement involving atomic oxygen) occur at the same grain boundaries, causing synergistic contributions to failure. In such a case the activation energy could be higher than 250 kJ/mol. This case should be rare in commercial alloys as such an alloy would show a very rapid increase of FCG rate with temperature, and using it would potentially be dangerous in case overheating of the part occurs, and would be eliminated from in alloy design.

Table 3. Activation energies for processes contributing to high temperature FCG. GB stands for grain boundary.

Processes contributing to high temperature FCG	Activation energy	
Single process		
Oxidation of carbides	~250 kJ/mol	
Dynamic embrittlement	~250 kJ/mol	
Grain boundary creep	~150 kJ/mol	
Change in static properties	$-\frac{mR_gT^2}{2}\frac{d\left(\ln\left(E\sigma_y\right)\right)}{d(T)}$ ~0 to 60 kJ/mol	
Mixed processes		
Dynamic embrittlement on GBs + creep of ligaments	~250 kJ/mol	
GB creep failure + oxidation dominated FCG	~150 to 250kJ/mol	
GB creep failure + non thermally activated failure	~0 to 150kJ/mol	

Fig. 4. Fatigue crack growth for several hypothetical scenarios (A, B, C): a) rate d*a*/d*N* and b) apparent activation energy.

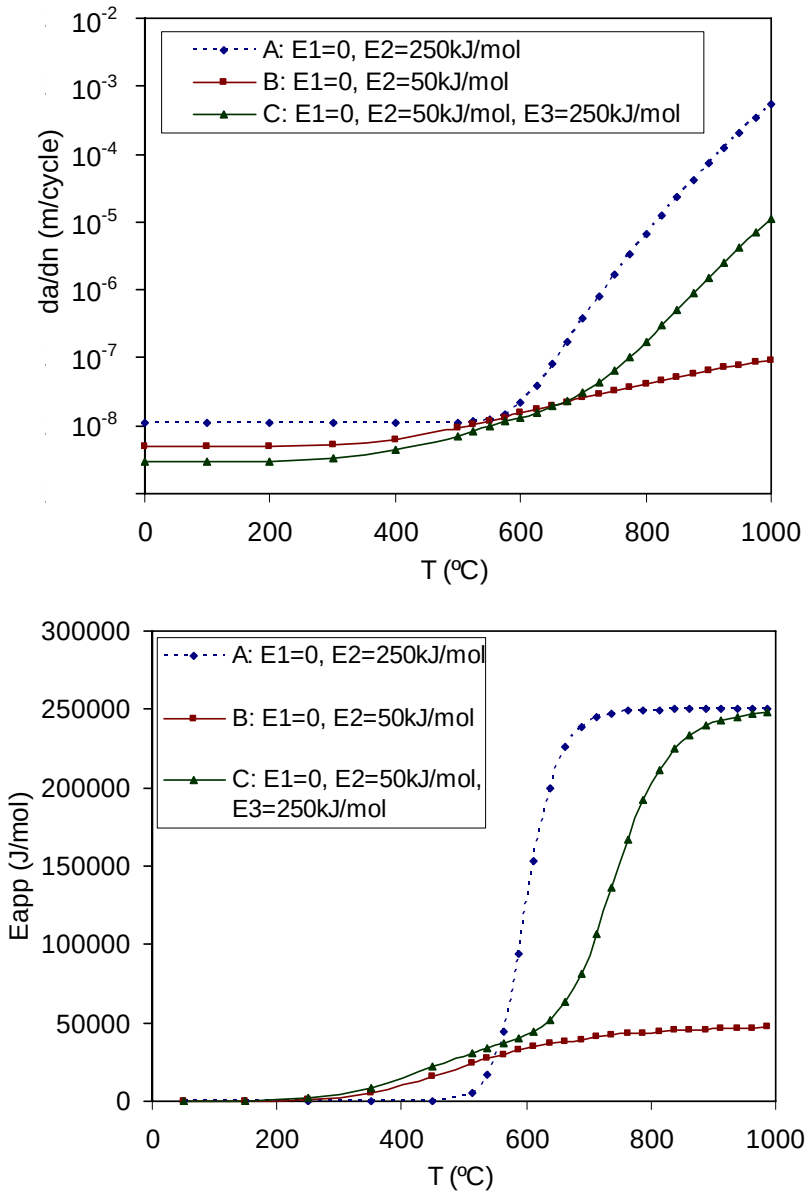

6. DISCUSSION

The mechanisms of FCG for the superalloys considered in the present paper as well as a range of other alloys have been discussed in a range of works, mostly on the basis of microstructural and post failure fractography data. The activation energy data in Fig. 2 and
Fig. **3**, and the comparison with expected activation energies for the various processes (Table 3), provides new insights with have not been available before. We will here consider the insights that can be obtained from this new analysis.

FCG processes are highly alloy dependent

First it is noted that the activation energies data in Fig. 2 and Fig. 3 are spread out over a wide range. Even if we limit the comparison to Ni based superalloys designed for one particular application (turbine discs) tested at similar temperatures (about 700ºC) with similar loading conditions (ΔK about 20 to 40MPa$\sqrt{m}$), activation energies vary from about 0 to about 300 kJ/mol. Following the analysis of activation energies in the previous paragraph, the large range of activation energies shows that for the various alloys different processes are rate determining. FCP in Ni based superalloys is thus seen to be highly multi-mechanistic, with large changes in the main rate determining mechanisms between the different alloys.

Evidence for oxidation dominated FCG in U720

The degradation of FCG resistance with increasing temperature for the U720Li variants for cycles including a dwell appears, in a qualitative sense, to be consistent with oxidation being a dominant process. Comparison of tests in air and vacuum shows that of the tests on U720Li variants and RR1000 reported in Fig 2, the 1-20-1-1 tests show the largest change in FCG rate between air and vacuum tests. Especially at low ΔK the difference is very large: nearly a factor of 100. This indicates that in those test conditions oxidation is the dominant process, and hence the activation energies measured for the 1-20-1-1 tests in the U720Li variants, which are about around 250 to 350kJ/mol, should be related to FCG dominated by oxidation. We can thus conclude when FCG is dominated by oxidation, the activation energy is about 250 to 350kJ/mol. However, the apparent activation energies of U720Li LG and U720Li for 1-1-1-1 cycles are substantially lower (80-100kJ/mol), indicating that oxidation either provides a much more limited or no contribution to the failure processes.

Evidence for elimination of thermal activation of FCG in latest generation of disc alloys

The activation energies for FCG in air for RR1000 and N18 are much lower than any known diffusion process (at grain boundaries or in the bulk) and apparent activation energies for FCG in the U720Li variants and the Inconels. The activation energies for RR1000 and N18 also show a clear decreasing trend with increasing ΔK, and activation energies become nearly zero for ΔK=50MPa$\sqrt{m}$. It is thought that these observations indicate that oxidation or creep is not the rate determining step in FCG for medium to high ΔK. (This is not to say the oxidation does not occur, it means that the oxidation that occurs is not significantly enhancing FCG.) In this case, where higher crack growth rates occur, pure cyclic (or mechanical) fatigue processes may be considered to predominate.

Consistent with the above analysis, the apparent activation energy for FCG is reduced to zero for testing in vacuum of RR1000. The graphical presentation of activation energies through a radar plot (Fig. 2) allows some direct observations about relative importance of mechanisms. In a single figure

this shows directly that at temperatures between 650 and 725 ºC: i) RR1000 is superior under all four testing conditions, ii) oxidation is not the rate determining process for FCG in RR1000, iii) for U720Li (the smaller grain variant studied here) oxidation related FCG is dominant for tests in air with a dwell, iv) U720Li LG is somewhat less prone to oxidation related FCG when compared to U720Li. The figure also suggests issues that would need further confirmation through other tests: v) there is no significant change in the main mechanism for FCG for the two U720Li variants when atmosphere is changed from air to vacuum in the absence of a dwell.

Microstructural factors influencing differences in thermal activation of FCG

One important aspect causing the differences between the Inconels and the U720Li variants on the one hand and RR1000 and N18, is the addition of Hf to the RR1000 and N18 alloys and Ta to the RR1000 alloy. These elements can influence FCG resistance in several ways. Firstly, the removal of Nb present in some Inconels, will remove the detrimental effect of oxidation of NbC. Ta is known to improve the creep resistance and fatigue crack growth resistance of Ni based superalloy turbine disks [55], and it has been suggested [55] that this is due to it entering the gamma-prime phase and improving the stability of the gamma-prime phase. Ta may also reduce local oxidation as it is generally used to substitute for Ti in γ' ($Ni_3(Al,Ti,Ta)$) thus potentially limiting the formation of Ti oxides. For fatigue resistance it is important that Hf and Ta elements will modify the MC carbides to become enriched in Hf and Ta, and under certain conditions MC carbides with a wide range of compositions from Hf lean (Ti,Ta)C to Hf rich MC can form [56]. The presence of these carbides containing Hf and Ta has been linked to increased oxidation resistance at small angle grain boundaries and an improved fatigue strength [57]. One mechanism through which Hf and Ta influence the grain boundaries is through the decomposition of the MC carbides during heat treatment and exposure at high temperatures, which will cause the formation of lower carbides such as the Cr-rich $M_{23}C_6$ carbides which form predominantly at grain boundaries. In the course of this transformation the local γ' content also changes through the reaction [58]:

MC ((Ti,Ta,Hf)C) + γ (Ni,Cr,Mo) -> $M_{23}C_6$ ($(Cr,Mo)_{23}C_6$) + γ' ($Ni_3(Al,Ti,Ta)$)

As C diffusion is orders of magnitude faster than diffusion of metallic alloying elements, and Ta and Hf diffusion is particularly slow, the rate of $M_{23}C_6$ and γ' formation is dependent mostly on the decomposition rate of the Ta and Hf containing MC carbides. Thus, in combination with heat treatment schedule, Ta and Hf additions offer the possibility of fine tuning the $M_{23}C_6$ and γ' distribution on grain boundaries. In addition, the MC carbides will to some extent be located preferentially at grain boundaries, because they slow down grain growth. These particles at grain boundaries are expected to influence fatigue crack propagation along grain boundaries [59] through two mechanisms. Firstly, formation of substantial amounts of the Cr-rich $M_{23}C_6$ carbides at grain boundaries will cause local Cr depletion of the matrix at the grain boundaries and hence cause changes in local susceptibility to oxidation. This effect is to some extent counteracted by the

increased Mo content of RR1000 and N18, which will substitute for some of the Cr in the formation of $(Cr,Mo)_{23}C_6$. On the other hand, the presence of carbides at grain boundaries will reduce creep by grain boundary sliding, and this effect is especially important for finer grained alloys. Thus carbides at grain boundaries will improve FCG resistance in vacuum and can improve FCG resistance in air provided the detrimental effect of Cr depletion at grain boundaries is kept limited. It has been stated that the composition and heat treatment of RR1000 is optimised to provide the optimum grain boundary carbide distribution with optimum size of carbide grain boundary particles of 350 to 550 nm [60]. On the basis of the present discussion it is suggested that the very low activation energy for FCG of RR1000 is related to a (near) optimised combination of heat treatment and Ta and Hf additions which produces an optimised distribution of fine carbides at grain boundaries. Apparently, this alloy optimisation has suppressed grain boundary oxidation and local creep to the extent that they are of limited importance for FCG at temperatures up to 725ºC. N18 also has a low apparent activation energy (Fig. 2), indicating suppression of oxidation related fatigue, but FCG resistance at 650ºC is not as good as that of RR1000 [31]. This may be caused by resistance to mechanical fatigue in N18 being less that that of RR1000.

Influencing of stress intensity on thermal activation of FCG

Fig. 2 shows that for several alloys the activation energy is dependent on stress intensity factor, ΔK. A range of mechanisms may be responsible. Firstly it can be noted that increasing ΔK will tend to reduce the influence of any OICC that may occur. As OICC will cause a negative contribution to E_{app}, increasing ΔK in conditions where OICC plays a role will cause an increase in apparent activation energy. This may play a role in the RR1000 1-20-1-1 test in air. If FCG is dominated by creep, a reduction in E_{app} with increasing ΔK through a reduction in jog formation energy is possible (see Eq. 7). This mechanism can potentially explain the reduction in E_{app} with increasing ΔK for RR1000 1-1-1-1 test in vacuum in Fig. 2 .

We may further note that if thermally activated processes are dominant at low ΔK, then increasing ΔK will tend to increase the relative importance of pure mechanical fatigue. Under such conditions we would expect a high E_{app} at low ΔK, which would decrease (towards 0) for increasing ΔK. This may be (part of) the explanation of the reduction of E_{app} with increasing ΔK for U720Li 1-20-1-1 tests in air.

Concluding remarks

The present paper contains an assessment of the method using FCP data currently available, linking them to processes that are currently understood to a reasonable extent. It is envisaged that as further reliable FCP data becomes available, further analysis can and will reveal further insights. This and more systematic linking of obtained E_{app} to post failure investigations will be the object of future work.

SUMMARY

A method for deriving apparent activation energies for fatigue crack growth (FCG) is presented. The apparent activation energies for FCG in air and vacuum, and with and without a dwell are obtained for several Ni based superalloys for turbine disc applications. The apparent activation energies range from zero to about 300kJ/mol. The apparent activation energies are used to analyse the main underlying mechanisms causing the progression of the crack. The analysis indicates that some alloys are prone to FCG through diffusion controlled mechanisms, notably grain boundary oxidation or creep, whilst other alloys are nearly immune to FCG grain boundary oxidation or creep. The apparent activation energy technique presented here offers a complementary approach to detailed micromechanistic evaluations based on observations and analysis of failed samples under a range of testing conditions. The present approach allows alternative assessments of which mechanisms may be contributing under the range of possible conditions, and this can allow more explicit evaluation of the changes in failure mechanism.

ACKNOWLEDGEMENTS

Thanks are due to QinetiQ Ltd., Farnborough, UK for financial support. Mr S. Everitt (University of Southampton, UK and QinetiQ) is gratefully acknowledged for performing FCG tests on N18. Dr J.W. Brooks (QinetiQ, Farnborough, UK), Dr N. Hide (formerly University of Southampton), Dr H.T. Pang (formerly University of Southampton, currently Cambridge University, UK), Dr I.M. Wilcock (formerly of QinetiQ, currently DSTL, Porton Down, Salisbury, UK), and Dr M.B. Henderson (formerly of QinetiQ, currently Industrial Research, New Zealand) are gratefully acknowledged for useful discussions and for performing part of the FCG tests presented in this paper. Rolls Royce plc are thanked for original materials supply of RR1000.

REFERENCES

1 S. Suresh, Fatigue of Materials, Cambridge University Press, 1991
2 H. Toda, I. Sinclair, J.Y. Buffiere, E. Maire, K.H. Khor, P. Gregson, T. Kobayashi, Acta Mater. 52 (2004) 1305-1317
3 T.F. Morgeneyer, M.J. Starink, I. Sinclair I, Acta Mater in press
4 N.Y. Yang and A. Plumtree, Mater Sci Eng A141 (1991) 55-61
5 M.B. Cortie and G.G. Garrett, Metall Trans A 19A (1988) 2979
6 W.J. Baxter, D.R. Lesuer and C.K. Syn, Metall Mater Trans A 31A (2000) 63
7 T. Connolley, P.A.S. Reed and M.J. Starink, Mater. Sci. Eng. A 340 (2003) 130-145
8 C.J. McMahon, Scripta Mater 54 (2006) 305-307.
9 J.A. Pfaendtner, C.J. McMahon, Acta Materialia 49 (2001) 3369-3377.
10 U. Krupp, W.M. Kane, C. Laird, C. J. McMahon, Mater. Sci. Eng. A 387-389 (2004) 409-413.
11 T. Goswami, H. Hanninen, Mater. Design 22 (2001) 217-236.
12 D. Fournier, A. Pineau, Metall. Trans. A 8A (1977) 1095–1105
13 E. Andrieu, R. Molins, H. Ghonem, A. Pineau, Mater. Sci. Eng. A 154 (1992) 21-28.

14 Longzhou Ma, Keh-Minn Chang, Scr. Mater. 8 (2003) 1271-1276.
15 H. Ghonem, T. Nicholas, A. Pineau. Fatigue Fract. Eng. Mater. Struct. 16 (1993) 577.
16 N.J. Hide, M.B. Henderson, and P.A.S. Reed, in Superalloys 2000, Proc of 9th Inter. Symposium on Superalloys, Sept 17-21, 2000, Seven Springs, Pennsylvania, ed. T.M. Pollock, R.D. Kissinger, R.R. Bowman, K.A. Green, M. McLean, S. Olson and J.J. Scirra, TMS (The Minerals, Metals and Materials Society, ASM), 495-503
17 A.M. Tucker, M.B. Henderson, A.J. Wilkinson, N.J. Hide, P.A.S. Reed, Mater. Sci. Techn. 18 (2002) 349-353
18 Y.L. Lu, L.J. Chen, P.K. Liaw, G.Y. Wang, C.R. Brooks, S.A. Thompson, J.W. Blust, P.F. Browning, A.K. Bhattacharya, J.M. Aurrecoechea, D.L. Klarstrom, ,Mater. Sci. Eng. A 429, (2006) 1-10.
19 C.F. Miller, G.W. Simmons, R.P. Wei, Scr. Mater. 48 (2003) 103-108..
20 S. Vyazovkin, Thermochim. Acta 355 (2000) 155.
21 M.J. Starink, Thermochim. Acta 404 (2003) 163-176.
22 E.J. Mittemeijer, J. Mater. Sci. 27 (1992) 3977.
23 I.N. Khan, M.J. Starink, J.L. Yan, Mater. Sci. Eng. A 472 (2008) 66-74.
24 T.G. Langdon, Scripta Mater. 35 (1996) 733
25 M.J. Starink, Int. Mater. Rev. 49 (2004) 191-226.
26 P.A.S. Reed, A. Wisbey, S. Everitt, I. DiMartino, J.W. Brooks, Proc. of Parsons 2007, 7th International Charles Parsons Turbine Conference, 11-13 Sept. 2007, University of Strathclyde, Glasgow, UK, in press
27 H.T. Pang, P.A.S. Reed, Mater. Sci. Eng. A 448 (2007) 67-79
28 S.J. Hessell, W. Voice, A.W. James, S.A. Blackham, C.J. Small, M.R. Winstone, US Patent 5897718, 1999.
29 Xingbo Liu, Bruce Kang, Keh-Minn Chang, Mater. Sci. Eng. A 340 (2003) 8-14.
30 K.-M. Chang, US Patent 5393483, 1995
31 S. Everitt, M.J. Starink, H.T. Pang, I.M. Wilcock, M.B. Henderson, P.A.S. Reed, Mater. Sci. Techn. 23 (2007) 1419-1423
32 P. Valerio, M. Gao, R. P. Wei, Scr. Metall. Mater. 30 (1994) 1269-1274.
33 K. Sadananda, P.J. Shahinian, Eng. Mater. Techn. 100 (1978) 381-387.
34 R.A. Swalin, A. Martin. J. Met. 206 (1956) 567.
35 R.C. Weast (Ed.), Handbook of Chemistry and Physics (66th ed.), CRC Press, Boca Raton, FL, USA (1985).
36 M.S.A. Karunaratne, R.C. Reed, Acta Mater. 51 (2003) 2905-2919.
37 S. K. Sondhi, B. F. Dyson, M. McLean, Acta Mater. 52 (2004) 1761-1772.
38 D. W. MacLachlan, D. M. Knowles, Mater. Sci. Eng. A 302 (2001) 275-285.
39 M.M. Shenoy, D.L. McDowell, R.W. Neu, Int. J. Plasticity 22 (2006) 2301-2326.
40 M.S. Lewandowski, R.A. Overfelt, Acta Mater. 47 (1999) 4695-4710.
41 M.F. Ashby, R.A. Verrall, Acta Metal. **21** (1973) 149–163.
42 J.H. Gittus, J. Eng. Mater. Tech. 99 (1977) 244–251.
43 M. Oktay Alniak, Fevzi Bedir, Mater. Sci. Eng. A 429 (2006) 295-303.
44 X.J. Wu, S. Yandt, P. Au, J.-P. Immarigeon, ASTM Special Technical Publication 1428 (2003) 3-14.
45 A.H. Cottrell, Dislocations and plastic flow in crystals, Clarendon Press (1953).
46 M. Gao, S.-F. Chen, G.S. Chen, R.P. Wei, ASTM Special Technical Publication 1297 (1997) 74–84.
47 S. Shimada, F, Yunazar, J. Am. Ceram. Soc. 83 (2000) 721–728.
48 S. Shimada, Solid State Ionics 141-142 (2001) 99-104.
49 S. Shimada, M. Inagaki, Sol. State. Ionics, 63-65 (1993) 312-317.
50 R Peraldi, D. Monceau, B. Pieraggi, Rev de Metall. 102 (2005) 136
51 Ali P. Gordon, Matthew D. Trexler, Richard W. Neu, Jr, Thomas J. Sanders, David L. McDowell, Acta Mater., In Press
52 S.D. Antolovich, S. Liu, R. Baur, Metall Mater Trans A 12 (1981) 473–481
53 G.A. Osinkolu, G. Onofrio, M. Marchionni, Mater Sci Eng. A 356 (2003) 425-433.
54 N. Kamp, N. Gao, M.J. Starink, M.R. Parry, I. Sinclair, ,Int. J. Fatigue 29 (2007) 897-908.
55 K.R. Bain, E.S. Huron, E.E. Montero, D.P. Mourer, P.L. Reynolds, J.J. Schirra, US Patent 6521175, 2002.
56 M.J. Starink, H. Cama, R.C. Thomson, Scr. Mater. 38 (1997) 73-80.
57 M. Konter, M. Newnham, C. Tonnes, US Patent 5759301, 1998.
58 M.J. Starink, R.C. Thomson, J. Mater. Sci. 36 (2001) 5603-5608.
59 Longzhou Ma, Keh-Minn Chang, Sarwan K. Mannan, Shailesh J. Patel, Scr. Mater. 48 (2003) 551-557.
60 A.J. Manning, D. Knowles, C.J. Small, US Patent Application 20020041821, 2002.